Journal of Materials and Environmental Science
ISSN : 2028-2508
CODEN : JMESCN

J. Mater. Environ. Sci., 2025, Volume 16, Issue 4, Page 720-737

http://www.jmaterenvironsci.com

Theoretical and experimental simulation to evaluate the inhibition activity of new nitroimidazole derivatives on copper corrosion in H_3PO_4 solution

Mougo André Tigori[1]*, Aboudramane Koné[1], N'guadi Blaise Allou[2], Simplice Koudjina[3,4], Kouassi Francesco Adingra[2], Drissa Sissouma[2], Paulin Marius Niamien[2]

[1]*Department of Mathematics, Physics and Chemistry, University of Jean Lorougnon Guede, BP 150 Daloa Daloa, Ivory Coast*
[2] *Laboratory of Constitution and Reaction of Matter, University of Felix Houphouet Boigny, 22 BP 582 Abidjan 22 Abidjan, Ivory Coast*
[3]*National High School of Applied Biosciences and Biotechnologies (ENSBBA), National University of Sciences, Technologies, Engineering and Mathematics (UNSTIM), Abomey, Sogbo-Aliho, Benin, |BP 486 Abomey, Sogbo-Aliho – Benin*
[4]*Laboratory of Chemical Physics-Materials and Molecular Modeling (LCP3M), University of Abomey- Calavi (UAC), 03 BP 3409 Cotonou – Benin*

**Corresponding author* tigori20@yahoo.fr

Received *05 Mar 2025,*
Revised *07 Apr 2025,*
Accepted *08 Apr 2025*

Keywords:
- ✓ *Inhibition activity;*
- ✓ *Initroimidazole derivatives;*
- ✓ *Orthophosphoric acid;*
- ✓ *Mass loss technique;*
- ✓ *Density functional theory*

Citation*: Tigori M.A., Koné A., Allou N.B., Koudjina S., Adingra F.F., Sissouma D., Niamien P.M. (2025) Theoretical and experimental simulation to evaluate the inhibition activity of new nitroimidazole derivatives on copper corrosion in H_3PO_4 solution, J. Mater. Environ. Sci., 16(4), 720-737*

Abstract: This study analyzes the inhibition activity of four nitroimidazole derivatives on copper corrosion in orthophosphoric acid. The activity of these compounds : 2-(2-(4-chlorobenzylidene)hydrazinyl)-3-nitroimidazo[1,2-a]pyridine (CHNP), 2-(2-(3-cyanobenzylidene)hydrazinyl)-3-nitroimidazo[1,2-a]pyridine (CYNP), 2-(2-(3-bromobenzylidene)hydrazinyl)-3-nitroimidazo[1,2-a]pyridine (BNP), and 2-(2-(2,4-dichlorobenzylidene)hydrazinyl)-3-nitroimidazo[1,2-a]pyridine (DNP), were evaluated using the mass loss technique and density functional theory (DFT) with B3LYP functional and 6-311G(d,p) base set. It was observed that the inhibition effect of these compounds intensified with the combined increase in concentration and temperature. Experimental results show that inhibition efficiency (IE) follows the following order: IE (CYNP) > IE (DNP) > IE (BNP) > IE (CHNP). Thus, CYNP stands out for its remarkable inhibition activity, reaching a maximum efficiency of 98.11% at 323 K and at a concentration of 2.10^{-4} M. The inhibition activity of these compounds is closely linked to their ability to donate and accept electrons from copper. The nucleophilic sites of this class of molecules, which are mainly made up of heteroatoms, and the electrophilic sites, mainly represented by carbon atoms, play a key role in their action mechanism.

1. Introduction

Nitrimidazoles are organic compounds derived from imidazole, widely used in medicine and biology for their antimicrobial and anticancer properties (Crowell *et al*., 2003; Upcroft *et al*.,2006). However, the use of certain organic and inorganic compounds as metal corrosion inhibitors has raised concerns in recent years, not least because of their potential toxicity (Milošev *et al*., 2016; Namitha *et al*., 2024; Arrousse *et al*., 2021; Hammouti *et al*., 2011; Karra *et al*., 2025). The application of these inhibitors in various industrial sectors, such as aeronautics, automotive, agriculture and pipelines, requires effective protection of metal equipment while minimizing environmental impacts. Contemporary research is therefore focusing on corrosion inhibitors that are less toxic, environmentally friendly and biodegradable. This concern has led researchers to explore the anticorrosive properties of various plant extracts and therapeutic compounds (Gasparac *et al.*,2000; Shubhra *et al.*, 2019; Jmiai *et al.*,2021; Lanzhou *et al.*, 2020; Oubahou *et al.*, 2024).

More recently, bibliometric analyses have been emerged to discover more information about the scope of research, collaboration between countries and institutions, most prolific authors, and emerging research (Huan and Guan, 2020; Xiao and Li, 2021; Aichouch *et al., 2025*). In this focus, a bibliometric analysis can be conducted on “corrosion & imidazole” to show the prolific authors, the most cited papers as well as the countries published on the use of imidazole derivatives as corrosion inhibitors. **Figure 1** exposed the evolution of publication against the years from 1981 to 2024. During this period, 721 papers were collected using Scopus. The number of publications increases to reach 90 in 2024. The most published authors are: Kokalj (Solovenia, 20 papers), Stupnišek-Lisac (Croitia, 17 papers), Rbaa (Morocco, 16), Zarrouk (Morocco, 14), Galai (Morocco, 12), Lakhrissi (Morocco, 12), Guo (China, 11), Ouakki (Morocco, 11), etc (**Figure 2**). The most cited paper belongs to Bereket *et al.*, (2002), with more 330 citations.

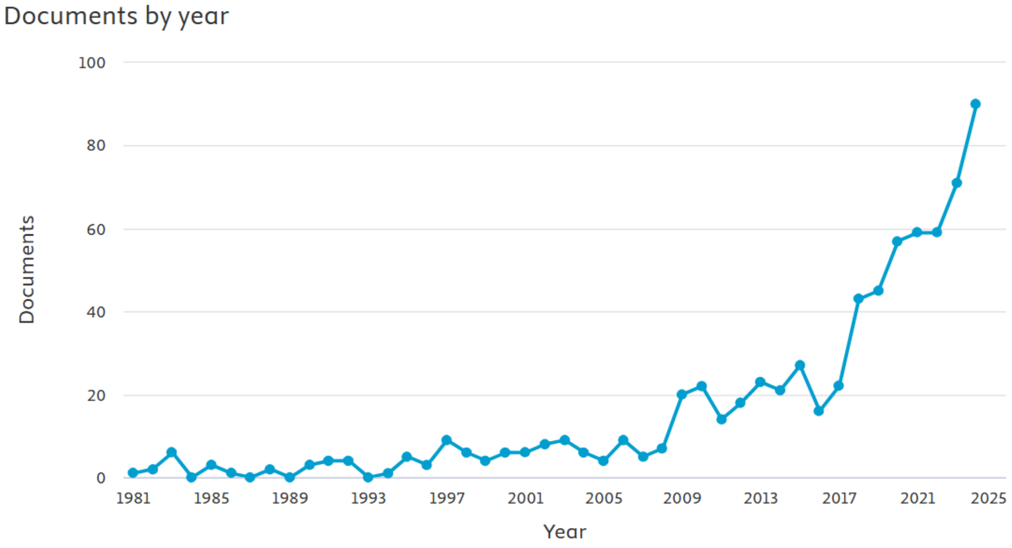

Figure 1: Evolution of publication against the years (1981-2024)

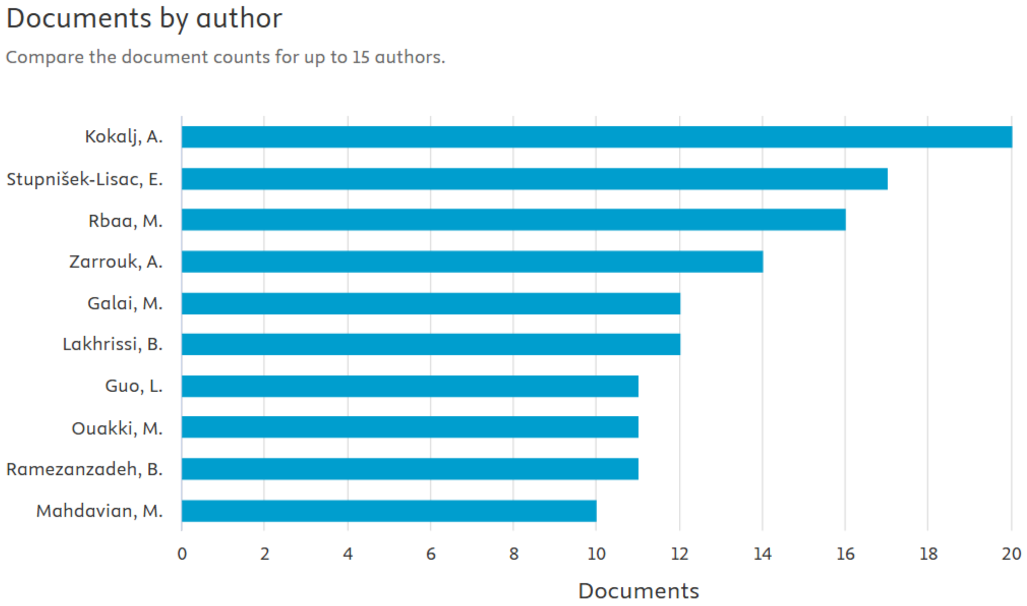

Figure 2: Classification of the most published authors

The affiliation comparison indicates that Ibn Tofail university is the most published (72 papers), followed by the Chinese Academy of Science (38 papers), and University of Zagreb (26 papers) … But China is the first published (245 papers); India (90 papers), Saudi Arabia (58), Morocco (57) and US (52). The VOS viewer indicates also the formation of teams shown by circles at different colors (**Figure 3**). The Moroccan researchers at four colors (Zarrouk indicated by blue node, Rbaa (pink), Hammouti (Green) and Ebn Touhami (Orange)) and each color visualize the cluster (group of authors in collaboration)

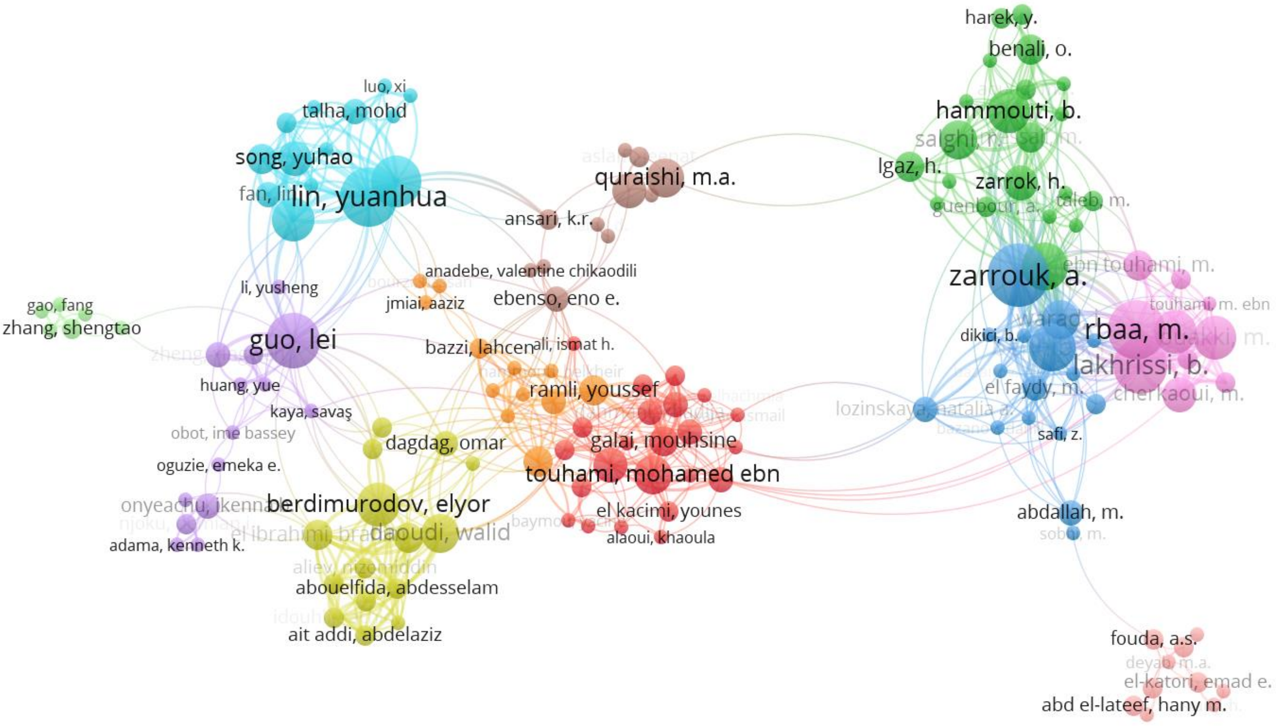

Figure 3: Author’s clusters via VOS viewer

With this in mind, four imidazole derivatives were tested in this work to assess their corrosion-inhibiting capabilities. These tests were carried out in a solution of orthophosphoric acid, a fluid commonly used in industry for operations such as descaling pipes and cleaning metal equipment, but which also exposes such equipment to corrosion (Spainhour *et al*., 2014). Damage caused by this phenomenon can result in considerable replacement costs. Furthermore, it is crucial to protect materials such as copper in order to prevent production stoppages and ensure infrastructure safety (Zarrouk *et al*., 2012; Hualiang *et al*., 2020). In the field of metal corrosion inhibition, several approaches are used. Among them, density functional theory (DFT), derived from computational chemistry, is proving to be a powerful tool. It relies on sophisticated computational methods and tools, such as numerical simulations and mathematical models, to analyze reaction mechanisms and interpret experimental results (Mohamed *et al*., 2018; Saha *et al*., 2015). This approach permits to resolve the chemical ambiguities associated with organic compounds and predict their behavior on metal surfaces. The tool is particularly valuable as it offers the possibility of exploring with great precision the molecular compounds reactivity in situations where direct experimentation would be complex or costly (Gökhan and Semra B *et al*., 2009). The aim of this study is to establish a correlation between the molecular properties of imidazole derivatives and their effectiveness as copper corrosion inhibitors in orthophosphoric acid.

2. Material and Methods

2.1 Synthesis mechanism of the molecules used

The four molecules used in our study were synthesized and analyzed by a team from the Matter Constitution and Reaction Laboratory at University of Felix Houphouët-Boigny, Ivory Coast. The synthesis mechanism is illustrated by the reaction diagram in **Figure 4.**

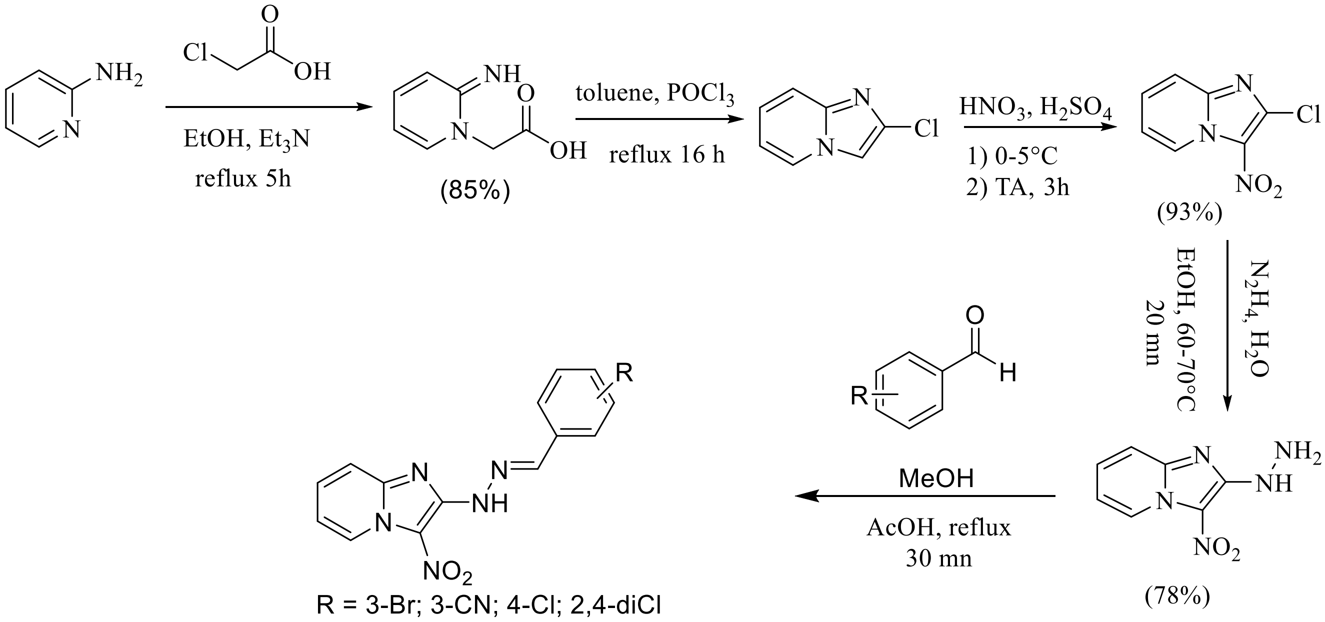

Figure 4. Synthesis procedure of imidazole derivatives used

2.2 Weight loss test

Cylindrical copper samples, 1 cm high and 0.25 cm in diameter, were initially weighed (m_1) using an analytical balance. These samples were then immersed in 50 ml of 2M orthophosphoric acid solution, either with or without an imidazole derivative at the desired concentration. Four concentrations 6.10^{-5}M, 9.10^{-5}M, 10^{-4}M, 2.10^{-5}M derived from the different inhibitors were prepared from 2M H_3PO_4. After one hour (1h), the samples were removed from the solution, brushed, rinsed thoroughly with distilled water, dried and reweighed (m_2). This procedure was carried out at two separate temperatures, 298 K and 323 K. Weight loss ($\Delta m = m_1 - m_2$) was then determined. From these measurements, copper corrosion rate (w) and inhibition efficiency (IE) of each molecule were calculated according to appropriate relationships:

$$w = \frac{m_2 - m_1}{St} \qquad \textbf{Eqn. 1}$$

$$IE(\%) = \frac{w_0 - w}{w_0} \times 100 \qquad \textbf{Eqn. 2}$$

w_0 et w (expressed in $g.cm^{-2}.h^{-1}$) are respectively the corrosion rate in the absence and presence of the molecule studied, S is the total surface area of copper sample and t is the immersion time.

2.3 Computation details

DFT calculations were performed using Gaussian 09W software (Frisch *et al.*, 2009), using B3LYP functional and 6-311G(d,p) basis set (Becke, 1993; Lee *et al.*, 1988). These functional uses approximations such as the local density approximation (LDA) and the generalized gradient approximation (GGA) (Becke, 1988). The molecular structures of the various compounds were optimized using GaussView 5.0 (**Table 1**). This method is based on idea that energy of a quantum system can be determined by its electron density, rather than by the full wave function, which simplifies calculations while providing highly accurate results. Quantum chemical calculations are based on Kohn-Sham equations, a set of single-particle equations that describe electrons in an effective potential (Kohn and Sham, 1965). These equations permit to determine the electron density that minimizes total energy of the system (Perdew, 1986). The chemical parameters of global reactivity obtained from these DFT calculations include total energy (E_T), highest occupied molecular orbital energy (E_{HOMO}), lowest unoccupied molecular orbital energy (E_{LUMO}), energy gap (ΔE), dipole moment (μ), ionization energy (I), electron, affinity (A), electronegativity (χ), global hardness (η), global softness (σ), electrophylicity index (ω), the fraction of electrons transferred between the inhibitor molecule (ΔN). The mathematical equations used to calculate these quantum descriptors are shown below. (Rajesh *et al.*, 2018), (Mohammed *et al.*, 2024), (Žaklina *et al.*, 2021) (Kumar *et al.*, 2019):

$$I = -E_{HO} \qquad \textbf{Eqn. 3}$$

$$A = -E_{\mathrm{BV}} \qquad \textbf{Eqn. 4}$$

$$\Delta E = E_{\mathrm{BV}} - E_{HO} \qquad \textbf{Eqn. 5}$$

$$\mu_P = \left(\frac{\partial E}{\partial N}\right)_{v(r)} = -\chi \qquad \textbf{Eqn. 6}$$

$$\chi = \frac{I+A}{2} = -\frac{E_{BV} + E_{HO}}{2} \qquad \textbf{Eqn. 7}$$

$$\sigma = \frac{1}{\eta} = \frac{2}{I-A} \qquad \textbf{Eqn. 8}$$

$$\eta = \frac{I-A}{2} = \frac{E_{BV} - E_{HO}}{2} \qquad \textbf{Eqn. 9}$$

$$\omega = \frac{\mu_P^2}{2\eta} = \frac{(\mathrm{I+A})^2}{4(\mathrm{I-A})} \qquad \textbf{Eqn. 10}$$

$$\Delta N = \frac{\chi_{Cu} - \chi_i}{2(\eta_{Cu} + \eta_{Cu})} \qquad \textbf{Eqn. 11}$$

In our study, the theoretical values of $\chi_{Cu} = 4.98\, eV$ (Pearson *et al.*, 1988) and hardness $\eta_{Cu} = 0$ (Pearson *et al.*, 1988) have been used for copper.

3. Results and Discussion

3.1 Weight loss analysis

Weight loss results were used to determine the inhibition efficiency (IE) of each compound. Table 2 and **Figure 5** Analysis shows that the inhibition efficiency of each compound increases with temperature and concentration. IE (CYNP) > IE (DNP) > IE (BNP) greater than IE (CHNP). It also emerges that the CYNP compound exhibits the highest inhibition efficiency at 323 K and at concentration of $C_{inh} = 2.10^{-4}$ M. This remarkable performance suggests that CYNP binds significantly to copper surface at high temperatures. This strong adsorption can be attributed to the cyanide group (-CN) presence in molecular structure.

Table 1. Compounds studied in this work.

Names	Molecular structure	Optimized structure
2-(2-(4-chlorobenzylidene)hydrazinyl)-3-nitroimidazo[1,2-a]pyridine (CHNP)	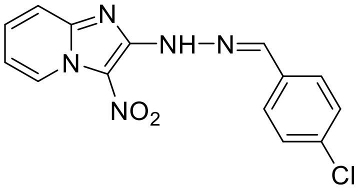	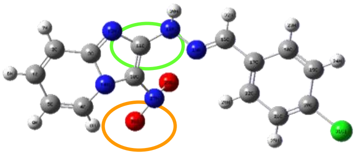
2-(2-(3-cyanobenzylidene)hydrazinyl)-3-nitroimidazo[1,2-a]pyridine (CYNP)	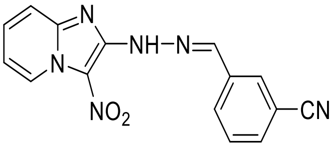	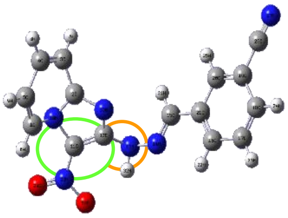
2-(2-(3-bromobenzylidene)hydrazinyl)-3-nitroimidazo[1,2-a]pyridine (BNP)	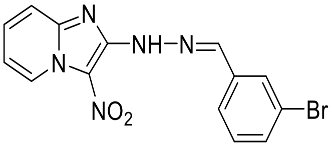	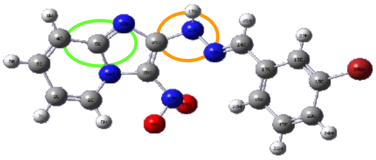
2-(2-(2,4-dichlorobenzylidene)hydrazinyl)-3-nitroimidazo[1,2-a]pyridine (DNP)	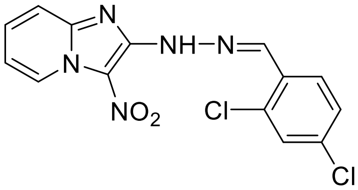	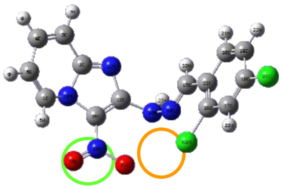

The different inhibition efficiency values of the molecules studied at 298K and 323K are listed in Table 2. These results are illustrated in **Figure 4**. Similar results have been obtained in the literature (Yujie *et al.*, 2019; Gadow *et al.*, 2019).

Table 2. IE values of the compounds studied

		IE(%)			
T(K)	C_{inh}(M)	CHNP	CYNP	BNP	DNP
298	6.10^{-5}	**28.71**	**42.85**	**31.42**	**35.71**
	9.10^{-5}	41.43	81.42	54.29	72.86
	10^{-4}	68.57	88.57	77.28	85.71
	2.10^{-4}	91.71	95.14	93.57	94.29
323	6.10^{-5}	61.11	77.78	64.44	72.22
	9.10^{-5}	76.67	89,89	77.78	87.78
	10^{-4}	82.22	93.71	85.55	92.22
	2.10^{-4}	**95.66**	**98.11**	**95.14**	**96.67**

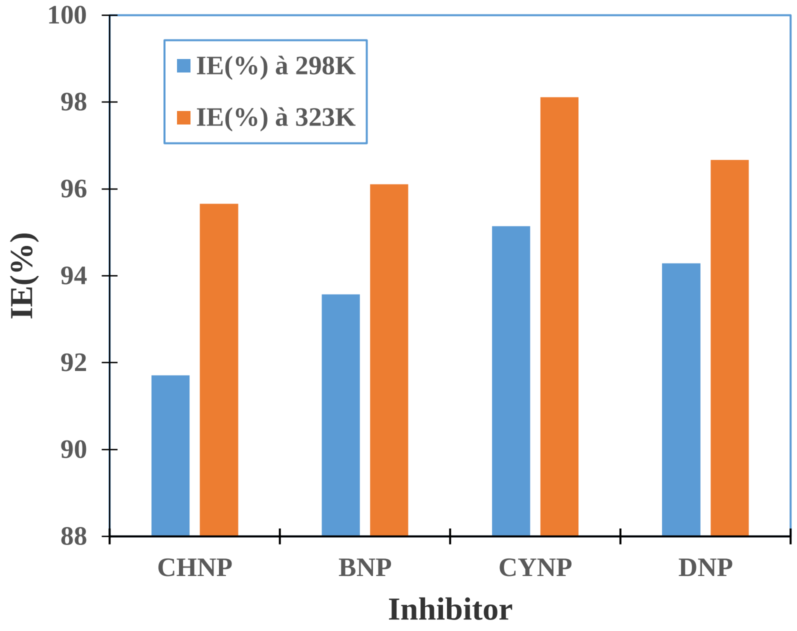

Figure 5. Evolution of IE for each inhibitor at 298 K and 323 K

3.2 Analysis of theoretical calculations

3.2.1 Correlation between global descriptors and inhibition efficiency

DFT calculations were used to determine global reactivity descriptors. The values of these descriptors are listed in **Table 3.** The ability of an organic compound to transfer electrons to a suitable acceptor is determined by the highest occupied molecular orbital energy (E_{HOMO}) (Yujie *et al.*,2017). Indeed, a high value of E_{HOMO} indicates a marked tendency of the compound to yield electrons to a suitable acceptor (Yujie *et al.*,2017). The order of E_{HOMO} values for the compounds studied is as follows: E_{HOMO} (CYNP) > E_{HOMO} (CHNP) > E_{HOMO} (BNP) > E_{HOMO} (DNP), suggesting that CYNP compound has the greatest propensity to transfer its electrons to copper, and may therefore be more adsorbed on its surface compared to the other compounds. These theoretical results agree with the experimental data. On the other hand, the lowest unoccupied molecular orbital energy (E_{LUMO}) of the compounds follows the order: E_{LUMO} (CHNP) < E_{LUMO} (DNP) < E_{LUMO} (BNP) < E_{LUMO} (CYNP). According to the literature, a low E_{LUMO} value indicates an increased capacity to accept electrons (Yujie *et al.*,2017), (Abdallah *et al.*,2021). Thus, CHNP and DNP compounds possess a high ability to accept electrons from copper, which can be attributed to the presence of chlorine in their structure. These electron transfers between the inhibitors and the metal suggest the formation of covalent bonds, promoting the creation of a protective layer on metal surface (Abdallah *et al.*,2021). HOMO and LUMO orbitals are shown in **Figure 6.**

The values of ionization energy (I) and electron affinity (A) corroborate the existence of strong interactions between each inhibitor and the metal. These intense interactions explain the compounds' excellent inhibition properties. Indeed, low ionization energy and high electron affinity values of the inhibitors reveal their instability, suggesting that these molecules are highly reactive. As for the energy gap (ΔE), the following order is observed: ΔE (CHNP) < ΔE (CYNP) < ΔE (DNP) < ΔE (BNP). The lower the energy difference between the highest occupied molecular orbital (HOMO) and the lowest unoccupied molecular orbital (LUMO), the greater the exchange between molecule and metal (El-Mokadem *et al.*, 2023; Bochuan *et al.*, 2020).

Table 3. Global reactivity descriptor values

Descripteurs quantiques	CHNP	CYNP	BNP	DNP
E_{HOMO} (eV)	-6.4467	-6.1314	-6.5574	-6.8071
E_{LUMO} (eV)	-3.7435	-2.4309	-2.4956	-2.9370
Energy gap ΔE (eV)	2.7032	3.7005	4.0618	3.8701
Dipole moment μ (D)	4.9905	3.6131	5.4077	7.2696
Ionization energy I (eV)	6.4467	6.1314	6.5574	6.8071
Electron affinity A (eV)	3.7435	2.4309	2.4956	2.9370
Electronegativity χ (eV)	5.0951	4.2812	4.5265	4.8721
global hardness η (eV)	1.3516	1.8503	2.0309	1.9351
Global softness σ $(eV)^{-1}$	0.7399	0.5405	0.4924	0.5168
Fraction of electron transferred ΔN	0.0426	0.1889	0.1117	0.0279
Electrophylicity index ω	9.6034	4.9530	4.0443	6.1335
Total energy E_T (Ha)	-1423.8901	-1056.4401	-3537.9119	-1883.4833

The values obtained show that the molecules studied are reactive, as the energy required to extract an electron from the last occupied orbital is relatively low. CHNP compound, with the lowest ΔE value, nevertheless shows the lowest inhibition activity. According to the literature, too small an energy gap, around 2.5 eV, is associated with an increased tendency of the molecule to lose or acquire electrons (Glaydson *et al.*, 2017). This phenomenon is not conducive to the stability of the layer formed on the metal, leading to a reduction in inhibition efficiency. On the other hand, molecules with an energy gap between 3.5 and 5 eV show the best inhibition activity, suggesting optimal reactivity, facilitated by the presence of several heteroatoms such as nitrogen and oxygen in their structure, which favors electronic exchange with the metal. These observations are corroborated by similar results in the literature (Abdelkader *et al.*,2014; Fateh *et al.*, 2020; Bochuan *et al.*, 2018; Bochuan *et al.*, 2019), and are consistent with experimental data.

Some researchers argue that low values of dipole moment (μ) favor the accumulation of inhibitor molecules on the metal surface, thus enhancing inhibition efficacy (Lingjie *et al.*,2012; Lei *et al.*,2014). Consequently, the low dipole moment values observed for the compounds may justify their high inhibition efficiency. CHNP compound, on the other hand, exhibits the highest softness value (σ) and the lowest hardness (η), suggesting that this molecule is softer and reacts more readily with copper to form a complex capable of reducing metal dissolution in the solution studied (Obot *et al.*,2010; Manilal *et al.*,2019). However, these theoretical results are not entirely consistent with experimental observations. Positive values for the fraction of electrons transferred and electronegativity indicate electron transfer between the inhibitors and the metal. The values of the fraction of electrons transferred (ΔN) are less than 3.6 and follow the following order: ΔN (CYNP) > ΔN (BNP) > ΔN (CHNP) > ΔN (DNP). These values justify the good inhibition performance of the molecules studied obtained experimentally (Tigori *et al.*,2022).

The highest ΔN value obtained with CYNP mentions that it adsorbs strongly to copper surface. This strong adsorption confirms its greater inhibiting power compared with the others. These data are consistent with experimental results. The high values of the electrophilicity index (ω) obtained confirm the electrophilic character of each inhibitor (Savaş *et al.*, 2016).

Inhibitors	Orbital HOMO	Orbital LUMO
CHNP	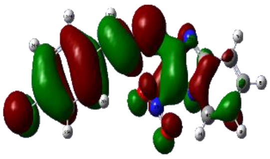	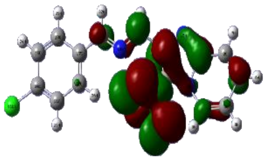
CYNP	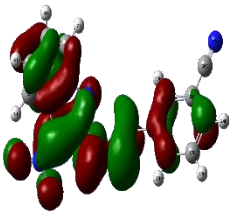	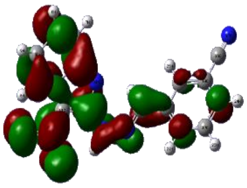
BNP	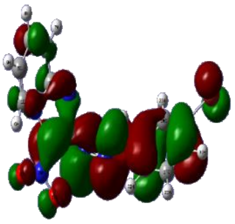	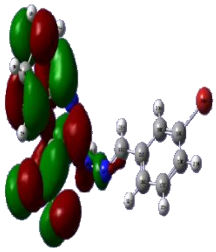
DNP	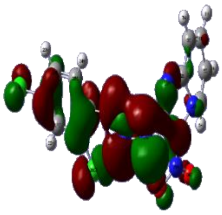	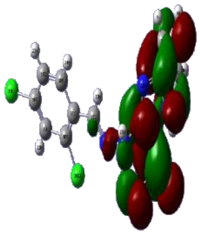

Figure 6. HOMO and LUMO orbitals of inhibitors

Consequently, these compounds are more likely to readily accept electrons from the metal or undergo nucleophilic attack. We observe that for each compound $\eta > 0$ and total energy (E_T), $E_T < 0$. The negative total energy values associated with each inhibitor suggest charge transfer from these molecules to the metal (Kumar *et al.*, 2019), implying favorable reactivity conducive to marked adsorption by each inhibitor to copper surface. CYNP has the highest total energy, indicating that the effectiveness of this compound lies in the process of charge transfer. This phenomenon enables the molecule to easily release electrons, which compensate for the electron deficit created in the copper when it dissolves in the acid. Similar observations have been made in previous studies (Sourav *et al.*,2015; Abdallah *et al.*,2022; Rashmi *et al.*, 2025).

3.2.1 Local reactivity

Local reactivity sites were identified using local reactivity descriptors. These descriptors, the Fukui and dual descriptor functions, were derived from Mulliken atomic charges. The mathematical relationships used to calculate these descriptors are expressed as follows (Damej *et al.*, 2021; Hualiang *et al.*, 2012):

- Nucleophilic attack

$$f_k^+ = q_k(N+1) - q_k(N) \qquad \textbf{Eqn. 12}$$

- Electrophilic attack

$$f_k^- = q_k(N) - q_k(N-1) \qquad \textbf{Eqn. 13}$$

$$\Delta f_k(\mathrm{r}) = f_k^+ - f_k^- \qquad \textbf{Eqn. 14}$$

Where $q_k(N+1)$, $q_k(N)$ et $q_k(N-1)$ are the electronic population of atomic sites k in $(N+1)$, N et $(N-1)$ electronic systems.

The values of these local reactivity parameters are given in **Table 4**, **5**, **6** and **7**

Table 4. Mulliken atomic charge values, f_k^+; f_k^- et $\Delta f_k(\mathrm{r})$ of CHNP

Atoms	$q_k(N+1)$	$q_k(N)$	$q_k(N-1)$	f_k^+	f_k^-	$\Delta f_k(\mathrm{r})$
1 C	-0.023016	-0.059576	0.007418	0.03656	-0.066994	0.103554
2 C	0.025551	-0.091978	-0.005503	0.117529	-0.086475	0.204004
3 C	0.011621	0.307045	0.019172	-0.295424	**0.287873**	**-0.583297**
4 C	-0.019097	0.050544	-0.005283	-0.069641	0.055827	-0.125468
5 C	0.071905	-0.157116	0.007254	0.229021	-0.16437	0.393391
6 H	0.000934	0.122357	-0.000556	-0.121423	0.122913	-0.244336
7 H	-0.001289	0.129347	0.000628	-0.130636	0.128719	-0.259355
8 H	0.000591	0.186666	-0.000731	-0.186075	0.187397	-0.373472
9 H	-0.003315	0.123137	-0.00051	-0.126452	0.123647	-0.250099
10 C	0.100311	0.294401	0.013172	-0.19409	0.281229	-0.475319
11 C	-0.000323	0.300321	0.044229	-0.300644	0.256092	-0.556736
12 N	0.234635	-0.260531	-0.003988	**0.495166**	-0.256543	**0.751709**
13 N	0.106591	-0.207597	-0.003631	0.314188	-0.203966	0.518154
14 H	0.046612	-0.338122	0.001974	0.384734	-0.340096	0.72483
15 N	0.015707	-0.353352	-0.009502	0.369059	-0.34385	0.712909
16 C	0.024101	0.11954	0.017005	-0.095439	0.102535	-0.197974
17 C	0.112706	-0.159174	-0.001964	0.27188	-0.15721	0.42909
18 C	0.007411	-0.063683	0.001685	0.071094	-0.065368	0.136462
19 C	0.002512	-0.016221	-0.00157	0.018733	-0.014651	0.033384
20 C	0.135906	-0.203686	0.005697	0.339592	-0.209383	0.548975
21 C	-0.01497	-0.006128	-0.003344	-0.008842	-0.002784	-0.006058
22 C	0.077829	-0.003701	0.010791	0.08153	-0.014492	0.096022
23 H	-0.001072	0.105775	-0.000096	-0.106847	0.105871	-0.212718
24 H	-0.000687	0.124433	0.000063	-0.12512	0.12437	-0.24949
25 H	-0.000056	0.132145	0.00016	-0.132201	0.131985	-0.264186
26 H	-0.004772	0.133758	-0.004656	-0.13853	0.138414	-0.276944
27 N	-0.016055	0.082426	0.283798	-0.098481	-0.201372	0.102891
28 O	-0.009827	-0.297765	0.300486	0.287938	-0.598251	**0.886189**
29 O	0.054269	-0.234143	0.329076	0.288412	-0.563219	0.851631
30 H	0.000352	0.211603	-0.00015	-0.211251	0.211753	-0.423004
31 Cl	0.066834	-0.054248	0.000158	0.121082	-0.054406	0.175488
32 H	-0.001901	0.083523	-0.001282	-0.085424	0.084805	-0.170229

Table 5. Mulliken atomic charge values, f_k^+; f_k^- et Δf_k(r) of CYNP

Atoms	$q_k(N+1)$	$q_k(N)$	$q_k(N-1)$	f_k^+	f_k^-	Δf_k(r)
1 C	-0.025201	0.064697	0.046944	-0.089898	0.017753	-0.107651
2 C	0.04184	0.350828	0.442186	-0.308988	-0.091358	-0.21763
3 C	0.018315	-0.082441	-0.080791	0.100756	-0.00165	0.102406
4 C	-0.015826	-0.075741	0.109146	0.059915	-0.184887	0.244802
5 C	0.09895	-0.109658	-0.040533	0.208608	-0.069125	0.277733
6 H	0.000712	0.164264	0.004146	-0.163552	0.160118	-0.32367
7 H	-0.000634	0.143532	0.015315	-0.144166	0.128217	-0.272383
8 H	0.000442	0.125819	-0.000988	-0.125377	0.126807	-0.252184
9 H	-0.003683	0.113821	0.001409	-0.117504	0.112412	-0.229916
10 N	0.064783	-0.443342	0.031408	0.508125	-0.47475	0.982875
11 C	0.264971	0.391924	-0.069345	-0.126953	**0.461269**	**-0.588222**
12 C	-0.073486	0.395754	0.098325	-0.46924	0.297429	-0.766669
13 N	0.278387	-0.402105	0.023502	**0.680492**	-0.425607	**1.106099**
14 N	0.223521	-0.302582	0.066986	0.526103	-0.369568	0.895671
15 C	-0.017045	0.166387	0.017084	-0.183432	0.149303	-0.332735
16 C	0.03734	-0.104376	0.103977	0.141716	-0.208353	0.350069
17 C	-0.014607	-0.092239	-0.031725	0.077632	-0.060514	0.138146
18 C	0.043824	-0.06472	0.06158	0.108544	-0.1263	0.234844
19 C	0.002771	0.049258	0.023431	-0.046487	0.025827	-0.072314
20 C	-0.003033	-0.106137	-0.008787	0.103104	-0.09735	0.200454
21 C	0.034282	0.061206	0.012152	-0.026924	0.049054	-0.075978
22 C	-0.001674	0.135194	-0.004979	-0.136868	0.140173	-0.277041
23 H	0.000393	0.114031	0.000978	-0.113638	0.113053	-0.226691
24 H	-0.001698	0.118132	-0.003236	-0.11983	0.121368	-0.241198
25 H	-0.000003	0.120758	0.00021	-0.120761	0.120548	-0.241309
26 C	-0.001597	0.278294	-0.00076	-0.279891	0.279054	-0.558945
27 N	0.003776	-0.460288	0.013948	0.464064	-0.474236	0.9383
28 N	-0.032557	0.299469	0.117739	-0.332026	0.18173	-0.513756
29 O	-0.014248	-0.362742	0.104035	0.348494	-0.466777	0.815271
30 O	0.0921	-0.447571	0.055423	0.539671	-0.502994	1.042665
31 H	0.015716	0.103747	-0.001807	-0.088031	0.105554	-0.193585
32 H	-0.00081	0.31429	0.001342	-0.3151	0.312948	-0.628048
33 N	-0.016021	-0.457462	-0.108314	0.441441	-0.349148	0.790589

The atom in the molecule with the highest values of f_k^+ and Δf_k(r) is more susceptible to nucleophilic attack. While the atom with the highest f_k^- and the value of Δf_k(r) is more prone to electrophilic attack.

Analysis of the various tables confirms that the atoms O (28), N (13), N (11) and N (14) are the likely sites for nucleophilic attack within the compounds CHNP, CYNP, BNP and DNP, respectively. These sites act as active electron capture centers. Each inhibitor can thus receive copper electrons from these sites. As for the electrophilic attack centers, the atoms capable of donating electrons to the metal in the CHNP, CYNP, BNP and DNP molecules are C (3), C (11), C (5) and C (28), respectively. These attack sites are shown in Table 1, where green and orange circles surround the centers for electrophilic and nucleophilic attacks respectively. It was observed that the nucleophilic sites of the molecules analyzed are made up of heteroatoms, which act as electron capture centers. These heteroatoms, which are oxygen and nitrogen, transfer their electrons to the carbon atoms within each molecule via the mesomer effect, making them electron-deficient. These electron-deficient centers then receive electrons from copper, while the carbon atoms, as electrophilic centers, transfer electrons to copper, which loses them during dissolution.

Table 6. Mulliken atomic charge values, f_k^+; f_k^- et $\Delta f_k(\mathrm{r})$ of BNP

Atoms	$q_k(N+1)$	$q_k(N)$	$q_k(N-1)$	f_k^+	f_k^-	$\Delta f_k(\mathrm{r})$
1 C	0.013066	0.06038	0.005511	-0.047314	0.054869	-0.102183
2 C	-0.01183	-0.161966	-0.002502	0.150136	-0.159464	0.3096
3 C	0.048721	-0.063311	0.005145	0.112032	-0.068456	0.180488
4 C	-0.010242	-0.094024	-0.001717	0.083782	-0.092307	0.176089
5 C	0.033556	0.310086	0.006338	-0.27653	**0.303748**	**-0.580278**
6 H	-0.000991	0.175389	0.003426	-0.17638	0.171963	-0.348343
7 H	0.000999	0.121327	0.000141	-0.120328	0.121186	-0.241514
8 H	-0.002551	0.120554	-0.00014	-0.123105	0.120694	-0.243799
9 H	0.001217	0.127213	0.000394	-0.125996	0.126819	-0.252815
10 N	0.003324	-0.3346	0.006314	0.337924	-0.340914	0.678838
11 N	0.200649	-0.279024	-0.003154	**0.479673**	-0.27587	**0.755543**
12 N	0.05614	-0.230419	0.006099	0.286559	-0.236518	0.523077
13 H	0.002208	0.209251	0.001237	-0.207043	0.208014	-0.415057
14 C	0.022335	0.129142	0.009062	-0.106807	0.12008	-0.226887
15 C	-0.051435	-0.101158	-0.001944	0.049723	-0.099214	0.148937
16 C	0.152345	-0.016883	0.006733	0.169228	-0.023616	0.192844
17 C	0.035692	-0.154904	-0.000647	0.190596	-0.154257	0.344853
18 C	-0.018576	-0.004693	0.000891	-0.013883	-0.005584	-0.008299
19 C	0.026171	-0.187417	-0.000819	0.213588	-0.186598	0.400186
20 C	0.103432	-0.031694	0.00371	0.135126	-0.035404	0.17053
21 H	0.001745	0.11959	0.000032	-0.117845	0.119558	-0.237403
22 H	-0.007514	0.140384	-0.004578	-0.147898	0.144962	-0.29286
23 H	0.000418	0.114711	0.000046	-0.114293	0.114665	-0.228958
24 H	-0.005247	0.121064	-0.000229	-0.126311	0.121293	-0.247604
25 C	-0.012439	0.28279	-0.006881	-0.295229	0.289671	-0.5849
26 C	0.282518	0.306481	0.045093	-0.023963	0.261388	-0.285351
27 N	-0.029901	0.075835	0.287286	-0.105736	-0.211451	0.105715
28 O	0.04248	-0.266193	0.259327	0.308673	-0.52552	0.834193
29 O	0.076992	-0.220479	0.374314	0.297471	-0.594793	0.892264
30 Br	0.048478	-0.002584	-0.000019	0.051062	-0.002565	0.053627
31 H	-0.001215	0.094217	0.000479	-0.095432	0.093738	-0.18917
32 N	-0.000546	-0.359067	0.001053	0.358521	-0.36012	0.718641

The carbon atoms that are the most likely sites for electrophilic attack share a double bond within each compound, enabling them to easily supply electrons to the copper. These electron transfers testify to the favorable interaction between each compound studied and copper. These observations explain the ability of the derivatives in question to effectively protect copper in acidic solution, during pickling and washing processes.

Table 7. Mulliken atomic charge values, f_k^+; f_k^- et $\Delta f_k(\mathrm{r})$ of DNP

Atoms	$q_k(N+1)$	$q_k(N)$	$q_k(N-1)$	f_k^+	f_k^-	$\Delta f_k(\mathrm{r})$
1 C	0.006487	0.040543	0.070008	-0.034056	-0.029465	-0.004591
2 C	0.003793	0.311201	0.11413	-0.307408	0.197071	-0.504479
3 C	0.00226	-0.090723	-0.039992	0.092983	-0.050731	0.143714
4 C	0.00919	-0.05888	0.151235	0.06807	-0.210115	0.278185
5 C	-0.003979	-0.153171	-0.047316	0.149192	-0.105855	0.255047
6 H	-0.000292	0.167955	-0.004843	-0.168247	0.172798	-0.341045
7 H	-0.000057	0.130688	0.001501	-0.130745	0.129187	-0.259932
8 H	-0.000189	0.125106	-0.009434	-0.125295	0.13454	-0.259835
9 H	0.000223	0.126398	0.001896	-0.126175	0.124502	-0.250677
10 N	-0.002345	-0.342557	0.067332	0.340212	-0.409889	0.750101
11 N	0.015706	-0.341721	-0.056296	0.357427	-0.285425	0.642852
12 C	0.000516	0.201446	0.126648	-0.20093	0.074798	-0.275728
13 N	0.270248	-0.260509	0.005494	0.530757	-0.266003	0.79676
14 N	0.399885	-0.228992	0.037668	**0.628877**	-0.26666	**0.895537**
15 C	-0.023757	0.151581	0.021096	-0.175338	0.130485	-0.305823
16 C	-0.001724	-0.149685	0.031367	0.147961	-0.181052	0.329013
17 C	0.005004	0.089397	-0.008149	-0.084393	0.097546	-0.181939
18 C	0.013523	-0.205165	0.041902	0.218688	-0.247067	0.465755
19 C	0.006491	-0.017696	-0.005957	0.024187	-0.011739	0.035926
20 C	-0.005966	-0.053603	0.0075	0.047637	-0.061103	0.10874
21 C	0.033181	-0.054345	0.015515	0.087526	-0.06986	0.157386
22 H	-0.000028	0.144438	0.000226	-0.144466	0.144212	-0.288678
23 H	-0.000444	0.125899	0.000153	-0.126343	0.125746	-0.252089
24 H	0.000115	0.111931	-0.000503	-0.111816	0.112434	-0.22425
25 H	0.016668	0.198554	0.001019	-0.181886	0.197535	-0.379421
26 Cl	0.17921	0.029862	0.002589	0.149348	0.027273	0.122075
27 Cl	0.010792	-0.043622	0.000602	0.054414	-0.044224	0.098638
28 C	0.021894	0.370905	0.025967	-0.349011	**0.344938**	**-0.693949**
29 N	-0.003356	0.109582	0.15499	-0.112938	-0.045408	-0.06753
30 O	0.000961	-0.237553	0.166616	0.238514	-0.404169	0.642683
31 O	0.020415	-0.281439	0.128567	0.301854	-0.410006	0.71186
32 H	0.025574	0.084176	-0.001532	-0.058602	0.085708	-0.14431

3. 3 Mechanism of inhibition action of compounds studied.

The reaction of orthophosphoric acid (H_3PO_4) is a triprotic acid, its dissociation in water follows the following steps:

$$H_3PO_4 \rightleftarrows H^+ + H_2PO_4^- \qquad \textbf{Eqn. 15}$$

$$H_2PO_4^- \rightleftarrows H^+ + HPO_4^{2-} \qquad \textbf{Eqn. 16}$$

$$HPO_4^{2-} \rightleftarrows H^+ + PO_4^{3-} \qquad \textbf{Eqn. 17}$$

The reaction of this acid with copper (Cu) can occur under a variety of conditions, often dictated by the cleaning and descaling processes used on metal pipes and equipment. This reaction can take place at ambient or elevated temperatures. Under these circumstances, copper in contact with orthophosphoric acid slowly dissolves to give Cu^{2+}, the reaction can be expressed as follows:

$Cu(s) + 2H^{+} \rightleftarrows Cu^{2+} + H_2$ **Eqn. 18**

Once Cu^{2+} ions have formed, they can react with phosphate ions to form complexes according to the balance shown below:

$3Cu^{2+}(aq) + 2PO_4^{3-} \rightarrow Cu_3(PO_4)_2$ **Eqn. 19**

At low temperatures, the corrosion rate of copper in this acid is generally low. However, as the temperature rises, the acid becomes more corrosive, favoring rapid dissolution of copper with the release of Cu^{2+}. The addition of a synthesized nitroimidazole derivative to the acid slows down this corrosion process, as shown by the experimental results. Indeed, in H_3PO_4 acid, each nitroimidazole compound (NI) is protonated and is in equilibrium with its corresponding neutral form (Gadow *et al.*, 2019), according to the following equation:

$3NI + H_3PO_4 \rightleftarrows 3[NIH]^{3+} + PO_4^{3-}$ **Eqn. 20**

The protonated form of each compound interacts with PO_4^{3-} leading to the formation of a protective layer resulting from electrostatic interactions between the charged species of the inhibitor and the hydrophosphate ions. This phenomenon corresponds to physisorption. The values of quantum chemical parameters such as ΔN, E_{HOMO}, E_{LUMO} and ΔE observed for each species studied indicate that these compounds can exchange electrons with copper via their reactive sites. These electron transfers are facilitated by the presence of heteroatoms (N, O) and π electrons of the aromatic rings in each compound. Indeed, each molecule has the capacity to supply electrons to empty copper orbitals and can also accept electrons from Cu^{2+}, thus forming coordination bonds (Raiedhah *et al.*, 2024**)**. The covalent bonds resulting from these exchanges enable each inhibitor to bind easily to copper surface, characterizing the phenomenon of chemical adsorption. This adsorption promotes the formation of a physical barrier on copper surface, which becomes increasingly robust as temperature and concentration increase, explaining the high inhibition efficiency values at higher temperatures.

Conclusion

A study of the activity of some nitroimidazole derivatives in the corrosion of copper in 2M orthophosphoric acid solution led to the following conclusions:

- Experimental data show that, for an appropriate concentration of 2.10^{-4} M, all four synthetic molecules exhibit notable inhibition activity at high temperatures. This shows that the presence of the cyanide (CN) group in CYNP compound promotes intense adsorption of the latter to the copper surface, conferring the best inhibition efficiency.
- Theoretical results from density functional theory (DFT) indicate that the heteroatoms (O, N) as well as π-bonds present in these derivatives facilitate electron exchange between the compounds and copper. This phenomenon testifies to the favorable reactivity of the compounds studied.
- The atoms O (28), N (13), N (11), and N (14) constitute the main sites for nucleophilic attacks, while the atoms C (3), C (11), C (5), and C (28) act as electrophilic attack centers in the respective compounds CHNP, CYNP, BNP and DNP.
- Substituents such as cyanide, chlorine and bromine influenced the inhibition activity of each compound studied.
- Theoretical results are in perfect agreement with experimental observations.

Acknowledgement: The authors would like to express their sincere gratitude to all the institutions that made this work possible.

Disclosure statement: *The authors declare that they have no conflicts of interest. With regard to ethics, this article does not present any research involving human or animal participants.*

Reference

Abdallah El A, Jmiai A., Moutie M. R, Rachid Oukhrib R, Abbiche K, Zejli H, Hilali M, Hassan B, Lahcen B, Souad El I. (2022) Computational and experimental studies of the inhibitory effect of imidazole derivatives for the corrosion of copper in an acid medium, *Journal of Molecular Liquids*, 345, 117813. https://doi.org/10.1016/j.molliq.2021.117813.

Abdallah M, Al Bahir A, Altass H.M., Fawzy A, El Guesmi N., Al-Gorair A. S, Benhiba F, Warad I, Zarrouk A. (2021) Anticorrosion and adsorption performance of expired antibacterial drugs on Sabic iron corrosion in HCl solution: Chemical, electrochemical and theoretical approach, *Journal of Molecular Liquids*, 330, 115702. https://doi.org/10.1016/j.molliq.2021.115702.

Abdelkader Z., Belkheir H., Dafali A., *et al.* (2014) A theoretical study on the inhibition efficiencies of some quinoxalines as corrosion inhibitors of copper in nitric acid, *Journal of Saudi Chemical Society*,18(5), 450-455. https://doi.org/10.1016/j.jscs.2011.09.011

Aichouch I., Kachbou Y., Bouklah M., Merimi C. (2025). Bibliometric analysis using VOSviewer: Analysis of Steel Corrosion using EIS, *J. Mater. Environ. Sci.* 16 (3), 411-421

Arrousse N., Salim R., Abdellaoui A., ElHajjaji F., *et al.* (2021), Synthesis, characterization, and evaluation of xanthene derivative as highly effective, nontoxic corrosion inhibitor for mild steel immersed in 1 M HCl solution, *Journal of the Taiwan Institute of Chemical Engineers,* 120, 344-359, https://doi.org/10.1016/j.jtice.2021.03.026

Becke A.D. (1988) Density-functional exchange-energy approximation with correct asymptotic behavior, *Physical Review*, 1988, 38, 3098-3100. https://doi.org/10.1103/PhysRevA.38.3098

Becke, A.D. (1993). Density-Functional Thermochemistry. III.The Role of Exact Exchange, *Journal of Chemical Physics*, 98,1372-1377. https://doi.org/10.1063/1.464913

Bereket G., Hür E., Öğretir C. (2002), Quantum chemical studies on some imidazole derivatives as corrosion inhibitors for iron in acidic medium, *Journal of Molecular Structure: THEOCHEM*, 578, Issues 1–3, 79-88, https://doi.org/10.1016/S0166-1280(01)00684-4

Bochuan T, Shengtao Z, Hongyan L, Yujie Q, Wenpo L, Lei G, Shijin C. (2019) Insights into the inhibition mechanism of three 5-phenyltetrazole derivatives for copper corrosion in sulfuric acid medium via experimental and DFT methods, *Journal of the Taiwan Institute of Chemical Engineers*,102,424-437. https://doi.org/10.1016/j.jtice.2019.06.005.

Bochuan T, Shengtao Z, Yujie Q, Lei G, Li F, Chaohui L, Yue X, Shijin C. (2018) A combined experimental and theoretical study of the inhibition effect of three disulfide-based flavouring agents for copper corrosion in 0.5 M sulfuric acid, *Journal of Colloid and Interface Science*, 526, 268-280. https://doi.org/10.1016/j.jcis.2018.04.092

Bochuan T, Shengtao Z, Yujie Q, Wenpo L, Hao L, Li F, Lei G, Chunliu X, Shijin C, Guangyi Z. (2020) Experimental and theoretical studies on the inhibition properties of three diphenyl disulfide derivatives on copper corrosion in acid medium, *Journal of Molecular Liquids*. 298,111975. https://doi.org/10.1016/j.molliq.2019.111975

Crowell A. L, Sanders-Lewis K. A, Secor W. E. 2003 In vitro metronidazole and tinidazole activities against metronidazole-resistant strains of *Trichomonas vaginalis*. *Antimicrob. Agents Chemother.* 47**,**1407-1409.

Damej M, Benmessaoud M, Zehra S., Kaya S, Hassane L, A. Molhi, N. L, El Hajjaji S., Awad A. A, Han-Seung. (2021) Experimental and theoretical explorations of S-alkylated mercaptobenzimidazole derivatives for use as corrosion inhibitors for carbon steel in HCl. *Journal of Molecular Liquids*, 331,115708. https://doi.org/10.1016/j.molliq.2021.115708

El-Mokadem T.H, Hashem A.I, Abd El-Sattar N. E.A, Dawood E.A, Abdelshafi N.S. (2023) Green synthesis, electrochemical, DFT studies and MD simulation of novel synthesized thiourea derivatives on carbon steel corrosion inhibition in 1.0 M HCl, *Journal of Molecular Structure*,1274(2),134567. https://doi.org/10.1016/j.molstruc.2022.134567.

Fateh A., Aliofkhazraei M, Rezvanian A.R. (2020) Review of corrosive environments for copper and its corrosion inhibitors, *Arabian Journal of Chemistry*, 135(1), 481-544. https://doi.org/10.1016/j.arabjc.2017.05.021.

Frisch M.J., Trucks G.W., Schlegel H.B., Scuseria G.E., Robb M.A., Cheeseman J.R., Scalmani G., Barone V., Mennucci B., Petersson G. A., Nakatsuji H., Caricato M., Li X., Hratchian H.P., Izmaylov A.F., Bloino J., *et al*., (2009). Gaussian 09. Gaussian, Inc., Wallingford, CT.

Gadow H.S, Thoraya A. F, Eldesoky A.M (2019) Experimental and theoretical investigations for some spiropyrazoles derivatives as corrosion inhibitors for copper in 2 M HNO3 solutions, *Journal of Molecular Liquids*, 294,111614.

Gasparac, R, Martin, C R, and Stupnisek-Lisac, E. (2000) In situ studies of imidazole and its derivatives as copper corrosion inhibitors. I. Activation energies and thermodynamics of adsorption. Journal of the Electrochemical Society ;147(2), 548-551. https://doi.org/10.1149/1.1393230

Glaydson L.F. M, Stefane N. C, Valder N. F, Paulo N.S. C, Adriana N. C, Pedro. (2017) Understanding the corrosion inhibition of carbon steel and copper in sulphuric acid medium by amino acids using electrochemical techniques allied to molecular modelling methods, *Corrosion Science*,115, 41-55. https://doi.org/10.1016/j.corsci.2016.11.012

Gökhan G., Semra B. (2009) Quantum chemical study of some cyclic nitrogen compounds as corrosion inhibitors of steel in NaCl media, *Corrosion Science*, 51(8), 1876-1878 https://doi.org/10.1016/j.corsci.2009.04.003.

Hammouti B., Zarrouk A., Al-Deyab S.S., Warad I. (2011), Temperature effect, activation energies and thermodynamics of adsorption of ethyl 2-(4-(2-ethoxy-2-oxoethyl)-2-p-tolylquinoxalin-1(4H)-yl)acetate on Cu in HNO_3, *Oriental J. Chem.* 27 N° 01, 23-31

Hualiang H, Furong B., Fan Z, Yongming T, Ziyi C, *et al*. (2012) Performance and theoretical study on corrosion inhibition of 2-(4-pyridyl)-benzimidazole for mild steel in hydrochloric acid, *Corrosion Science*, 61, 1-9, https://doi.org/10.1016/j.corsci.2012.03.045.

Hualiang H., Furong B. (2020) Correlations between the inhibition performances and the inhibitor structures of some azoles on the galvanic corrosion of copper coupled with silver in artificial seawater, *Corrosion Science*, 165,108413. https://doi.org/10.1016/j.corsci.2019.108413.

Jmiai A, Tara A, El Issami S, Hilali M., Jbara O, Bazzi L. (2021) A new trend in corrosion protection of copper in acidic medium by using Jujube shell extract as an effective green and environmentally safe corrosion inhibitor: Experimental, quantum chemistry approach and Monte Carlo simulation study, *Journal of Molecular Liquids*, 322, 114509, https://doi.org/10.1016/j.molliq.2020.114509

Karra D, Timoudan N, Bazanov D R., Lozinskaya N A., Zarrok H., Oudda H., Benmessaoud D L, Zertoubi M, Assouag M, Benhiba F, El Faydy M, Saranya J., Abuelizz H A., Zarrouk A. (2025) Corrosion inhibition performance of imidazole derivative for protection of carbon steel in hydrochloric acid solution: Experimental and theoretical analysis, International Journal of Electrochemical Science, 20(6),101015. https://doi.org/10.1016/j.ijoes.2025.101015

Kokalj A. (2021) On the alleged importance of the molecular electron-donating ability and the HOMO–LUMO gap in corrosion inhibition studies, *Corrosion Science*, 180,109016, https://doi.org/10.1016/j.corsci.2020.109016Kohn W, Sham L.J. (1965) Self-Consistent

Equations including exchange and Correlation Effects, *Physical Review*, 140, A1133-A1138. https://doi.org/10.1103/PhysRev.140.A1133

Kumar D., Nimesh J., Vinay J., Beena R. (2020) Amino acids as copper corrosion inhibitors: A density functional theory approach, *Applied Surface Science*, 514,145905. https://doi.org/10.1016/j.apsusc.2020.145905.

Lanzhou G., Shini P., Xiaomei H., Zhili G. (2020) A combined experimental and theoretical study of papain as a biological eco-friendly inhibitor for copper corrosion in H2SO4 medium. *Applied Surface Science*, 511, 145446. https://doi.org/10.1016/j.apsusc.2020.145446.

Lee, C., Yang, W. and Parr, R.G. (1988). Development of the Colle-Salvetti Correlation-Energy Formula into a Functional of the Electron Density, *Physical Review B*, 37, 785-789. https://doi.org/10.1103/PhysRevB.37.785

Lei G, Shanhong Z, Shengtao Z, Qiao H, Weihua L. (2014) Theoretical studies of three triazole derivatives as corrosion inhibitors for mild steel in acidic medium, *Corrosion Science*, 87, 366-375. https://doi.org/10.1016/j.corsci.2014.06.040.

Lingjie L, Xueping Z, Jinglei L, Jianxin H, Shengtao Z, Fusheng P. (2012), Adsorption and corrosion inhibition of Osmanthus fragran leaves extract on carbon steel, *Corrosion Science*, 63,82-90. https://doi.org/10.1016/j.corsci.2012.05.026

Manilal M, Sourav Kr. S, Naresh C. M, Priyabrata B. (2019) Effect of stereochemical conformation into the corrosion inhibitive behaviour of double azomethine based Schiff bases on mild steel surface in 1 mol L^{-1} HCl medium: An experimental, density functional theory and molecular dynamics simulation study, *Corrosion Science*, 146, 134-151. https://doi.org/10.1016/j.corsci.2018.10.002.

Milošev I; Kovačević N; Kokalj A (2016), Effect of Mercapto and Methyl Groups on the Efficiency of Imidazole and Benzimidazole-based Inhibitors of Iron Corrosion. *Acta Chimica Slovenica*,l 63(3),544 https://doi.org/10.17344/acsi.2016.2326

Mohamed M.M, Ahmed S.R, Basma G. (2018) Experimental and DFT insights into molecular structure and optical properties of new chalcones as promising photosensitizers towards solar cell applications, *Applied Surface Science*, 452, 337-351. doi.org/10.1016/j.apsusc.2018.05.007

Mohammed O, Mohamed R, Hassane L, Driss T, Youssef N, Awad A. A, Han-seung L. (2024). Exploring sustainable corrosion inhibition of copper in saline environment: An examination of hydroquinazolinones via experimental and ab initio DFT simulations, *Arabian Journal of Chemistry*,17(5),105716. https://doi.org/10.1016/j.arabjc.2024.105716

Namitha K, Padmalatha R, Suma A. R. (2024) Imidazole-based ionic liquid as sustainable green inhibitor for corrosion control of steel alloys: A review, *Journal of Molecular Liquids*, 411,125789, https://doi.org/10.1016/j.molliq.2024.125789

Obot I.B., Obi-Egbedi N.O.(2010) Theoretical study of benzimidazole and its derivatives and their potential activity as corrosion inhibitors, *Corrosion Science*,52(2), 657-660. https://doi.org/10.1016/j.corsci.2009.10.017

Oubahou M, El aloua A, Benzbiria N., *et al*. (2024). Electrochemical, thermodynamic and computational investigation of the use of an expired drug as a sustainable corrosion inhibitor for copper in 0.5 M H_2SO_4. *Materials Chemistry and Physics*,323, 129642. https://doi.org/10.1016/j.matchemphys.2024.129642

Pearson R.G. (1988) Absolute Electronegativity and Hardness: application to Inorganic Chemistry, *Inorganic Chemistry*, 27(4), 734-740.

Perdew J.P. (1986) Density-functional approximation for the correlation energy of the inhomogeneous electron gas, *Physical Review*, 33, 8822-8824. https://doi.org/10.1103/PhysRevB.33.8822

Raiedhah A. A., Medhat M. K, Mervate M. Mohamed A, Kame R.A, Mohamed M.M. (2024) Corrosion Inhibitionof Expired Cefazolin Drug on Copper Metal in Dilute Hydrochloric Acid Solution:

Practical and Theoretical Approaches, *Molecules*, 29,1157. https://doi.org/10.3390/molecules29051157

Rajesh H, Dwarika P, Akhil S, Raman K. (2018) Experimental and theoretical studies of Ficus religiosa as green corrosion inhibitor for mild steel in 0.5 M H_2SO_4 solution, *Sustainable Chemistry and Pharmacy*, 9, 95-105. https://doi.org/10.1016/j.scp.2018.07.002.

Rashmi S., Bindu M. (2025) Coordination interaction of biologically important macromolecules with metals and alloys for corrosion protection: An extensive study. *Coordination Chemistry Reviews*, 525, 216346. https://doi.org/10.1016/j.ccr.2024.216346.

Saha S.K., Ghosh P., Hens A., Murmu N.C, Banerjee P. (2015) Density functional theory and molecular dynamics simulation study on corrosion inhibition performance of mild steel by mercapto-quinoline Schiff base corrosion inhibitor, *Physica E: Low-dimensional Systems and Nanostructures*, 66,332–341. https://doi.org/10.1016/j. physe.2014.10.035

Savaş K, Burak T, *et al.* (2016), Determination of corrosion inhibition effects of amino acids: Quantum chemical and molecular dynamic simulation study, *Journal of the Taiwan Institute of Chemical Engineers*, 58, 528-535. https://doi.org/10.1016/j.jtice.2015.06.009.

Shubhra P, Deepti J, Shamima H, Amrita B, Rahul S, Saroj K. P, *et al.* (2019). A new insight into corrosion inhibition mechanism of copper in aerated 3.5 wt.% NaCl solution by eco-friendly Imidazopyrimidine Dye: experimental and theoretical approach, *Chemical Engineering Journal*, 358, 725-742, https://doi.org/10.1016/j.cej.2018.08.079.

Sourav Kr. S, Pritam G, Abhiram H, Naresh C.M, Priyabrata B. (2015) Density functional theory and molecular dynamics simulation study on corrosion inhibition performance of mild steel by mercapto-quinoline Schiff base corrosion inhibitor, *Physica E: Low-dimensional Systems and Nanostructures*, 66,332-341. https://doi.org/10.1016/j.physe.2014.10.035

Spainhour C.B. (2014). Phosphoric Acid,Editor(s): Philip Wexler,Encyclopedia of Toxicology (Third Edition), Academic Press,916-919. https://doi.org/10.1016/B978-0-12-386454-3.00904-0

Tigori M.A,Koné A, Souleymane B, Zon D, *et al.* (2022) Combining Experimental and Quantum Chemical Study of 2-(5-Nitro-1,3-Dihydro Benzimi-dazol-2-Ylidene)-3-Oxo-3-(2-Oxo-2H-Chromen-3-yl) Propanenitrile as Copper Corrosion Inhibitor in Nitric Acid Solution, *Open Journal of Physical Chemistry*, 12, 47-70. https://doi.org/10.4236/ojpc.2022.124004

Upcroft J. L, Wright J.B. K, Upcroft P, Vanelle P. (2006) 5-Nitroimidazole Drugs Effective against Metronidazole-Resistant Trichomonas vaginalis and Giardia duodenalis, *Antimicrob Agents Chemother*, 50(1), 344-347. https://doi.org/10.1128/aac.50.1.344-347.2006

Yujie Q, Shengtao Z, Lei G, Xingwen Z, Bin X, Shijin C. (2017). Experimental and theoretical studies of four allyl imidazolium-based ionic liquids as green inhibitors for copper corrosion in sulfuric acid, *Corrosion Science*, 119, 68-78. https://doi.org/10.1016/j.corsci.2017.02.021

Yujie Q., Shengtao Z., Liping W. (2019) Understanding the adsorption and anticorrosive mechanism of DNA inhibitor for copper in sulfuric acid. *Applied Surface Science*. 492, 228-238. https://doi.org/10.1016/j.apsusc.2019.06.190.

Žaklina Z. T,Mihajlović M.B.P, Milan B. R,. Simonović A. T, Antonijević M.M. (2021) Experimental and theoretical studies of paracetamol as a copper corrosion inhibitor. *Journal of Molecular Liquids*, 327,114817. https://doi.org/10.1016/j.molliq.2020.114817.

Zarrouk A., Zarrok H., Salghi R., *et al.* (2012) A Theoretical Investigation on the Corrosion Inhibition of Copper by Quinoxaline Derivatives in Nitric Acid Solution, *International Journal of Electrochemical Science*,7(7), 6353-6364. https://doi.org/10.1016/S1452-3981(23)19486-7.
